Stochastic resonance in a trapping overdamped monostable system

N. V. Agudov,[1,*] A. V. Krichigin,[1] D. Valenti,[2] and B. Spagnolo[2,†]
[1]*Radiophysics Faculty, Nizhniy Novgorod State University, 23 Gagarin Avenue, 603950 Nizhniy Novgorod, Russia*
[2]*Dipartimento di Fisica e Tecnologie Relative, Group of Interdisciplinary Physics,[‡] Università di Palermo and CNISM-INFM, Viale delle Scienze, ed. 18, I-90128 Palermo, Italy*
(Received 6 November 2009; revised manuscript received 27 February 2010; published 18 May 2010)

The response of a *trapping* overdamped monostable system to a harmonic perturbation is analyzed, in the context of stochastic resonance phenomenon. We consider the dynamics of a Brownian particle moving in a piecewise linear potential with a white Gaussian noise source. Based on linear-response theory and Laplace transform technique, analytical expressions of signal-to-noise ratio (SNR) and signal power amplification (SPA) are obtained. We find that the SNR is a nonmonotonic function of the noise intensity, while the SPA is monotonic. Theoretical results are compared with numerical simulations.

DOI: 10.1103/PhysRevE.81.051123 PACS number(s): 05.40.−a, 02.50.Ey

I. INTRODUCTION

The dynamics of nonlinear periodically driven stochastic systems has attracted great attention during the last decades. The interest in these systems is much stimulated by the phenomenon known as stochastic resonance (SR), where noise plays a constructive role [1–3]. This effect consists of an enhancement of sensitivity of a nonlinear system to external periodical forcing due to random fluctuations. Nowadays the SR has been found and studied in different physical, chemical, and biological systems [4–15]. The enhancement of sensitivity is usually understood as nonmonotonic dependence of the signal-to-noise ratio (SNR), or the signal power amplification (SPA) at the output of nonlinear system, as a function of the input noise intensity. Accordingly, the phenomenon of SR displays itself when SNR or SPA reaches a maximum at some value of noise intensity and then decreases with further growth of fluctuations.

The effect of SR has been observed in various monostable systems: in a model system with multiplicative noise [16], in an array of monostable oscillators [17], in an underdamped single-well Duffing oscillator [18], in a harmonic oscillator with a weak nonlinearity at higher harmonics [19], in an overdamped nonlinear model system [20], and in a single metastable state to study the thermal instability in a superconducting stripline resonator [21]. Recently, considerable attention has been focused on Brownian motion in modulated optical trap [22–25] and in bistable confining potentials [26]. Specifically, in Ref. [22] the Brownian dynamics of an optically trapped water droplet was investigated across the transition from overdamped to underdamped regime, in Ref. [23] the suppression of noise in a noisy optical trap was theoretically and experimentally investigated, and in Refs. [24,25] the effects of a modulating laser field on the motion of an overdamped trapped Brownian particle were observed and theoretically described. However, most of the previous work is experimental one and there is a lack of theoretical investigation on the dynamics of trapped particle, subject to noise and modulated by an external driving field in a monostable system with a nonlinear potential profile.

Motivated by these studies we analyze the response of a *trapping* overdamped monostable stochastic system to a periodic signal, in the context of stochastic resonance phenomenon. Specifically we consider a Brownian particle moving in a piecewise linear potential in the presence of a white Gaussian noise source. Our starting point is the following Langevin equation

$$\frac{dx}{dt} = -\frac{\partial \Phi(x,t)}{\partial x} + \xi(t), \tag{1}$$

with

$$\Phi(x,t) = \Phi(x) - xs(t), \tag{2}$$

where $s(t)=A\cos(\omega_0 t+\varphi)$ is the input driving field, $\xi(t)$ is a white Gaussian noise source with the usual statistical properties: $\langle \xi(t)\rangle=0$, $\langle \xi(t)\xi(t+\tau)\rangle=2q\delta(\tau)$, and $2q$ is the noise intensity. Here, $\Phi(x)$ is the potential field describing the system and $x(t)$ is the position of the trapped Brownian particle.

The canonical example of SR was observed and studied in the overdamped system (1) for bistable potential profiles $\Phi(x)$ with single potential barrier separating the metastable states [1–3,27]. This result can be generalized for multistable potentials with arbitrary number of barriers. The value of additive noise intensity for which SNR reaches the maximum, by using an approximated expression for SNR [see Eq. (5.9) of Ref. [27]], may be expected at $2q \approx \Delta U$, with ΔU as the height of the potential barrier. In other words, the presence of potential barrier(s) has been considered as necessary condition for arising of SR in overdamped systems with additive noise, except threshold systems, where the SR phenomenon is known to be present. It is well known also that in bistable (multistable) systems the nonmonotonic dependence of SNR on noise intensity is accompanied by nonmonotonic behavior of SPA.

Recently, in Ref. [28] it was shown that some special kind of SR can appear in overdamped monostable systems (1), where no barrier is present in potential profile $\Phi(x)$. This kind of SR can coexist with the conventional SR if the sys-

*agudov@rf.unn.ru
†spagnolo@unipa.it
‡http://gip.dft.unipa.it

 ©2010 The American Physical Society

tem is multistable. The authors find a nonmonotonic dependence on the noise intensity only for SPA. In very recent investigations on stochastic resonance in overdamped monostable systems with different piecewise linear potential profiles [29,30] it was shown analytically that the SPA and SNR can have monotonic or nonmonotonic behavior, as a function of the noise intensity, strongly depending on the potential profiles.

In the present paper we show that the nonmonotonic dependence of SNR, similarly to that observed for bistable systems, can be found also in monostable overdamped systems with a trapping nonlinear potential profile. This result implies the presence of SR-like phenomenon in monostable overdamped systems driven by a periodic field and a white noise source. The paper is organized as follows. In the next section the theoretical approach, based on linear-response theory (LRT) and Laplace transform technique with the analytical expressions of SNR and SPA, is presented. In the third section the comparison between the analytical results and numerical simulations obtained by integration of Eq. (1), together with the probability distributions (PDs) of the particle position is shown. In the final section we draw the conclusions.

II. THEORETICAL APPROACH

Consider the following piecewise linear monostable potential

$$\Phi(x) = \begin{cases} k_1|x|, & |x| < L \\ k_2(|x| - L) + k_1 L, & |x| > L. \end{cases} \tag{3}$$

This potential profile is monostable and is characterized by two parameters specifying the slope of potential profile wells: k_1 describes the slope near the minimum for $|x|<L$ and k_2 for $|x|>L$. Both values k_1 and k_2 are always positive, providing the monostability (single minimum) of the potential $\Phi(x)$, while k_1 can be greater than k_2 and vice versa. For $k_1 \gg k_2$ we have a trapping monostable potential (TMP), while for $k_1 \ll k_2$ we get a *confining* monostable potential.

Due to the presence of the periodical driving force in Eq. (1), the potential profile of Eq. (3) takes different configurations in time. In Fig. 1 we show these configurations at three different times, $t=0, T/4, T/2$, with $T=(2\pi)/\omega_0$, for the following parameter values of the potential profile: $k_1=20$, $k_2=1$, $L=0.1$, corresponding to a trapping potential.

To obtain the power spectrum density (PSD) of the output signal $x(t)$, the LRT is used assuming that the magnitude A of the driving signal $s(t)$ is small enough, namely, $A \ll \min\{k_1, k_2\}$. In accordance with LRT [2], the PSD of the output process $x(t)$ is

$$S_x(\omega) = S_x^{(0)}(\omega) + \frac{a^2}{4}[\delta(\omega - \omega_0) + \delta(\omega + \omega_0)]. \tag{4}$$

The function $S_x^{(0)}(\omega)$ provides the noise platform and the other term is the power spectral density due to the output signal with amplitude a. Therefore, the SNR is defined as follows [2]:

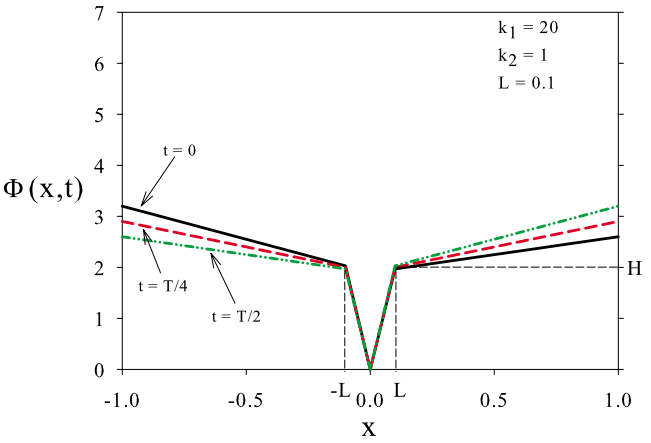

FIG. 1. (Color online) Trapping piecewise linear monostable potential $\Phi(x,t)$ [see Eqs. (2) and (3)] for the following set of parameter values: $k_1=20$, $k_2=1$, and $L=0.1$. Amplitude and frequency of the periodical forcing are $A=0.3$ and $\omega=0.1$, respectively. The potential is shown at three different times: $t=0$ (black solid line), $t=T/4$ (red long dashed line), and $t=T/2$ (green medium dashed-dotted line), with $T=2\pi/\omega_0$. The typical parameter of the potential profile is $H=k_1\ L=2$.

$$R = \frac{a^2}{2S_x^{(0)}(\omega_0)}. \tag{5}$$

The function $S_x^{(0)}(\omega)$ is the PSD of the unperturbed system (1) for $s(t)=0$ and is defined as the Fourier transform of the appropriate unperturbed autocorrelation function,

$$S_x^{(0)}(\omega) = \frac{1}{\pi}\int_0^\infty K_x^{(0)}[\tau]\cos(\omega\tau)d\tau, \tag{6}$$

where

$$K_x^{(0)}[\tau] = \langle x(t)x(t+\tau)\rangle. \tag{7}$$

In the above expression we have taken into account that $K_x^{(0)}[\tau]$ is an even function. According to the LRT, the amplitude of output signal is

$$a = A|\chi(i\omega_0)|, \tag{8}$$

where $\chi(i\omega)$ is the susceptibility of the system. Therefore, the SPA of the input signal $s(t)$ is

$$\eta = \frac{a^2}{A^2} = |\chi(i\omega_0)|^2. \tag{9}$$

The susceptibility is the Fourier transform of the linear-response function $h(\tau)$,

$$\chi(i\omega) = \int_{-\infty}^{\infty} h(\tau)e^{-i\omega\tau}d\tau, \tag{10}$$

while the linear-response function can be expressed in terms of correlation function of the unperturbed system in accordance with the fluctuation-dissipation theorem,

$$h(\tau) = -\frac{\theta(\tau)}{q}\frac{dK_x^{(0)}[\tau]}{d\tau}, \tag{11}$$

where $\theta(\tau)$ is the Heaviside function.

The probability density function (PDF) of the unperturbed process $W^{(0)}(x,t)$ satisfies the Fokker-Planck equation (FPE) [31],

$$\frac{\partial W^{(0)}(x,t)}{\partial t} = \frac{\partial}{\partial x}\left(\frac{d\Phi(x)}{dx}W^{(0)}(x,t) + q\frac{\partial W^{(0)}(x,t)}{\partial x}\right), \tag{12}$$

with boundary conditions $W^{(0)}(\pm\infty,t)=0$. Since we consider $\Phi(x)\to\infty$ with $x\to\pm\infty$, the stationary PDF,

$$W_{st}^{(0)}(x) = N\exp\left(-\frac{\Phi(x)}{q}\right), \tag{13}$$

will be established in the system with time. Here, N is the normalization factor. Therefore, to find the autocorrelation function,

$$K_x^{(0)}[\tau] = \int_{-\infty}^{\infty} x_0 W_{st}^{(0)}(x_0)dx_0 \int_{-\infty}^{\infty} xW^{(0)}(x,\tau|x_0)dx, \tag{14}$$

it is necessary to obtain the transition probability density $W^{(0)}(x,t|x_0)$, which is the solution of FPE (12) with the initial conditions $W^{(0)}(x,0)=\delta(x-x_0)$.

For real physical systems the integration in Eq. (10) has to be performed from zero, because linear-response function, according to Eq. (11), exists only if $\tau>0$. Therefore the susceptibility $\chi(i\omega)$ in Eq. (10) can be considered as the Laplace transform of the linear-response function,

$$\chi(p) = \hat{h}(p) = \int_0^{\infty} h(\tau)e^{-p\tau}d\tau, \tag{15}$$

where $p=i\omega$ is the Laplace variable. On the other hand, we can obtain the Laplace transform of the linear-response function by integrating expression (11). Finally, we get

$$\chi(i\omega) = \frac{1}{q}(K_x^{(0)}[0] - i\omega\hat{K}_x^{(0)}[i\omega]), \tag{16}$$

where $K_x^{(0)}[0]$ is the correlation function at $\tau=0$,

$$K_x^{(0)}[0] = \langle x^2\rangle + m_{st}^2, \tag{17}$$

which is expressed in terms of variance and mean value of the stationary distribution (13). The PSD (6) also can be written as the real part of the Laplace transform $\hat{K}_x^{(0)}[p]$,

$$S_x^{(0)}(\omega) = \frac{1}{\pi}\mathrm{Re}\{\hat{K}_x^{(0)}[i\omega]\}. \tag{18}$$

In the present paper the Laplace transform of the autocorrelation function is obtained for the monostable potential of Eq. (3). The Laplace transform method for the solution of the FPE is described in Refs. [32–35]. In particular, in Ref. [33] the exact Laplace transform of the transition probability density is obtained for piecewise linear potential profile consisting of an arbitrary number of linear parts. Using this approach we obtain the following exact expression for the Laplace transform of the unperturbed autocorrelation function:

$$\hat{K}_x^{(0)}[p] = \frac{\langle x^2\rangle}{p} + \frac{\sum_{i=0}^{9} A_i}{B}, \tag{19}$$

where $\langle x^2\rangle$ and the coefficients A_i and B have the following expressions:

$$\langle x^2\rangle = \frac{q}{2p\beta\delta^2}\frac{2+2h\delta+h^2\delta^2-(h^2+2h+2\lambda)\delta^3}{1-\lambda\delta}, \tag{20}$$

$$A_0 = \frac{4q\beta\lambda\mu(1-4\delta)}{(1-\lambda\delta)},$$

$$A_1 = -\frac{8q\beta(1-\delta)[(1-\lambda)\alpha_1^2+\alpha_2^2]\gamma_1}{(1-\lambda\delta)},$$

$$A_2 = \frac{2q[2\lambda\mu(2-\delta)-4\delta\mu+\delta\lambda(2-\mu)\gamma_1]}{(1-\lambda\delta)},$$

$$A_3 = -\frac{4q\gamma_1\{(2-\delta)\alpha_2^2+\delta\lambda[2+(2-\mu)\gamma_2]\}}{\delta^2(1-\lambda\delta)(1+\gamma_2)},$$

$$A_4 = -\frac{4q\gamma_1\alpha_1^2(2-3\delta)(1-\lambda)}{\delta^2(1-\lambda\delta)(1+\gamma_2)},$$

$$A_5 = \frac{2q\mu[(2-\delta)\lambda+2\delta(2-\lambda)\gamma_2+2\delta(1-\lambda)]}{\delta^2(1-\lambda\delta)(1+\gamma_2)},$$

$$A_6 = \frac{q\gamma_1(2-\mu)[\delta\lambda(1+\gamma_2)-6+2\delta-2\gamma_2]}{\beta\delta^2(1-\lambda\delta)(1+\gamma_2)},$$

$$A_7 = \frac{2q\mu[1+\delta(2-\lambda)-2\delta^2\lambda]\gamma_2}{\beta\delta^2(1-\lambda\delta)(1+\gamma_2)},$$

$$A_8 = \frac{2q\mu[3+4\lambda-2\delta^2\lambda-\delta(2+3\lambda)]}{\beta\delta^2(1-\lambda\delta)(1+\gamma_2)},$$

$$A_9 = \frac{4q\mu}{\beta^2\delta^3(1+\gamma_2)}, \tag{21}$$

$$B = p^2(1+\gamma_2)^2[(2-\mu)\gamma_2-\mu(1-\delta+\delta\gamma_2)]. \tag{22}$$

In Eqs. (20)–(22) $h=k_1L/q$, $\beta=k_1^2/2pq$, $\gamma_1=\sqrt{1+4pq/k_1^2}$, $\gamma_2=\sqrt{1+4pq/k_2^2}$, $\delta=k_2/k_1$, and

$$\lambda = 1-e^h, \quad \mu = 1-e^{h\gamma_1},$$

$$\alpha_1 = \sqrt{1-\mu}-\frac{1}{\sqrt{1-\lambda}}, \quad \alpha_2 = \sqrt{1-\mu}-\sqrt{1-\lambda}. \tag{23}$$

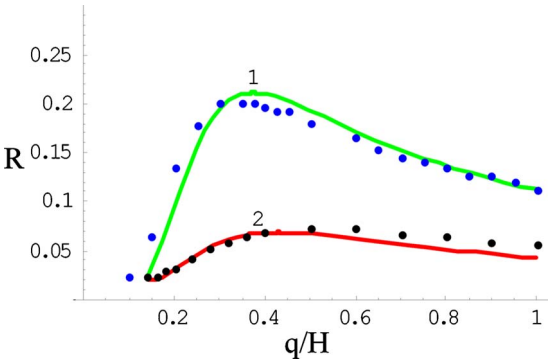

FIG. 2. (Color online) SNR [Eq. (5)] of the system output of Eq. (1) versus dimensionless noise intensity q/H, for the particle position $x(t)$ moving along the trapping monostable potential of Fig. 1. The amplitude and the frequency of the driving periodic field are $A=0.3$ and $\omega_0=0.1$, respectively. Curve 1 (green solid line) corresponds to $k_1=20$, $k_2=1$, $L=0.1$ (potential profile 1) and curve 2 (red solid line) corresponds to $k_1=25$, $k_2=3$, $L=0.2$ (potential profile 2). The solid lines are the theoretical results obtained from Eq. (5), while the dots are the results of simulations obtained by numerical integration of Eq. (1).

III. RESULTS: THEORETICAL ANALYSIS AND NUMERICAL SIMULATIONS

With the above analytical result [Eq. (19)] for the autocorrelation function, we can obtain the PSD [Eq. (18)] and the SNR [Eq. (5)]. In Fig. 2 the signal-to-noise ratio R is plotted versus the dimensionless input noise intensity q/H for two different sets of potential parameter values k_1, k_2, and L. We indicate as potential profile 1 that obtained setting in Eq. (3) $k_1=20$, $k_2=1$, $L=0.1$, and potential profile 2 that obtained setting $k_1=25$, $k_2=3$, $L=0.2$. We get curve 1 (green solid line) for potential profile 1 and curve 2 (red solid line) for potential profile 2. $H=k_1L$ is a parameter of the potential of Eq. (3), useful to define the trap (see Fig. 1). The amplitude and frequency of the periodical driving force are $A=0.3$ and $\omega_0=0.1$, respectively. As one can see from Fig. 2, for large q the SNR is a decreasing function of q, similarly to the other cases of monostable potentials considered earlier (see Ref. [29]). However, for intermediate values of noise intensity, namely, $0.1H \leq q \leq 0.5H$, a nonmonotonic behavior of the SNR appears. It looks similar to the effect of SR observed in bistable systems with barrier (see, for example, Refs. [1,2]).

In the same Fig. 2 the results of numerical simulations (full circles) are shown. In particular, the numerical SNRs have been obtained from Eq. (1), by calculating the time series for the position of the Brownian particle, and successively by using the fast Fourier transform technique [36]. The maximum simulation time is equal to $t_{max}=628$. The agreement between theoretical and numerical results is quite good. The properties of this SNR behavior depend on the parameter values of the investigated monostable potential of Eq. (3). The nonmonotonic behavior of SNR is observed when $k_1 > 6.25k_2$, as it results from numerical evaluation of Eqs. (5), (18), and (19). The maximum of SNR is reached at noise intensity $q^* \simeq 0.35H$ for curve 1 and $q^* \simeq 0.45H$ for curve 2. This maximum is more pronounced for the potential profile shown in Fig. 1 and characterized by very low pendency for $|x| > L$. In particular, for curve 1 in Fig. 2 we can note an enhancement in the SNR of about one order of magnitude, with noise intensity increasing from $q=0.1H$ to $q^* = 0.35H$.

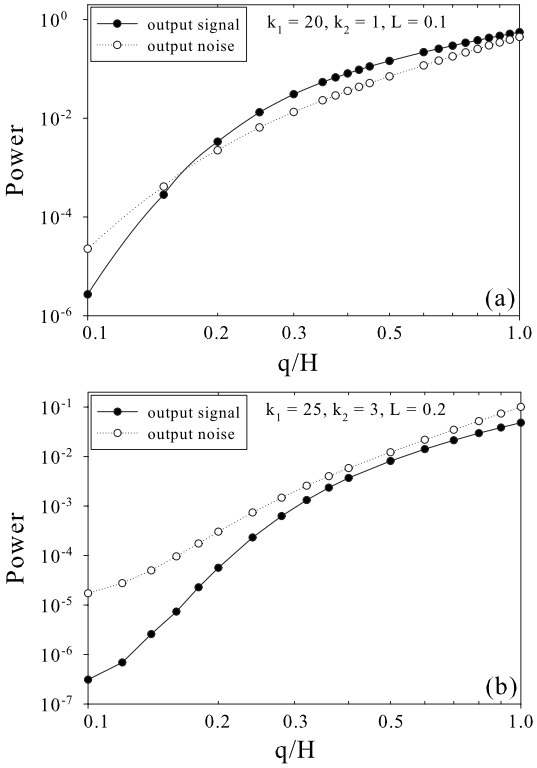

FIG. 3. Output signal power and output noise power as functions of dimensionless input noise intensity q/H for two potential profiles, as computed from numerical integration of Eq. (1). (a) Potential profile 1 ($k_1=20$, $k_2=1$, $L=0.1$); (b) potential profile 2 ($k_1=25$, $k_2=3$, $L=0.2$). The values of other parameters are the same as in Fig. 2.

In Fig. 3 we report the output signal power and the output noise power as functions of dimensionless input noise intensity q/H for potential profiles 1 and 2, as computed from numerical integration of Eq. (1). From inspection of these figures we see that in the low dimensionless noise intensity regime ($q < q^*$), the rate of increase of the output signal power exceeds the corresponding rate of the output noise power, while the opposite happens in the high dimensionless noise intensity regime ($q > q^*$). It is this change of rate in correspondence of q^* in both potential profiles that gives rise to the peak in the SNR behavior of Fig. 2.

In spite of the similar behavior shown by SNR in TMP and bistable systems, the mechanism of the SR observed in the TMP should be different from that occurring in bistable systems, where the key parameter of the SR effect is the height of potential barrier. In the considered monostable system there is no barrier; and the force, originating from the potential, always tends to push the Brownian particle toward the equilibrium point $x=0$, corresponding to the minimum of the potential profile of Eq. (3). The SR in TMP appears because of the special shape of the potential, which defines the

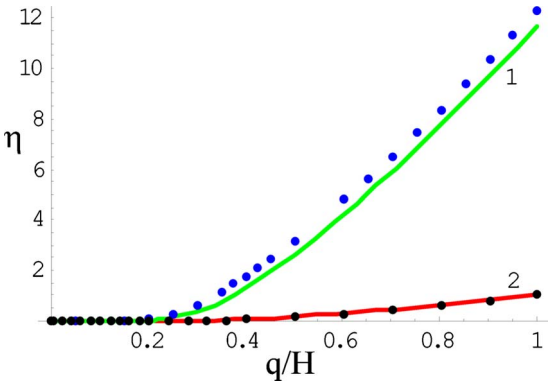

FIG. 4. (Color online) SPA [Eq. (9)] of the system output of Eq. (1) versus dimensionless noise intensity q/H, for the particle position $x(t)$ moving along the trapping monostable potential of Fig. 1. The amplitude and the frequency of the driving periodic field are $A=0.3$ and $\omega_0=0.1$, respectively. Curve 1 (green solid line) corresponds to $k_1=20$, $k_2=1$, $L=0.1$ (potential profile 1) and curve 2 (red solid line) corresponds to $k_1=25$, $k_2=3$, $L=0.2$ (potential profile 2). The solid lines are the theoretical results obtained from Eq. (9), while the dots are the results of simulations obtained by numerical integration of Eq. (1).

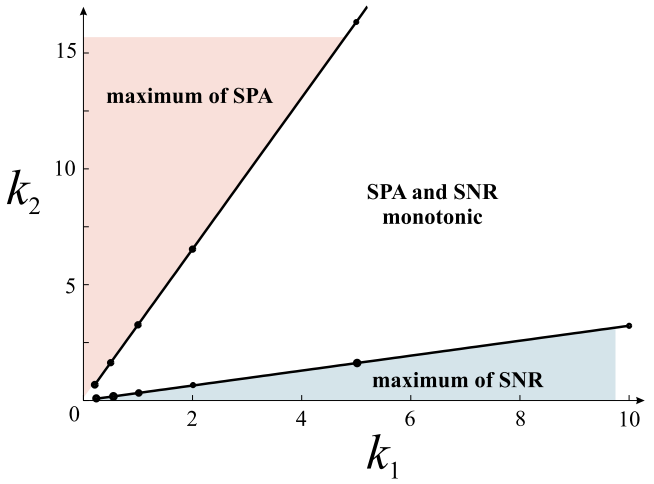

FIG. 5. (Color online) The two shaded areas of the parameter space (k_1,k_2) indicate the regions where maximum of SPA or SNR can be observed. The amplitude and the frequency of the driving periodic field are $A=0.3$ and $\omega_0=0.1$, respectively. In the monostable system of Eq. (3), the maximum of SPA is observed for $k_1<0.305k_2$ $(k_2>3.27k_1)$, corresponding to confining monostable potentials; while the maximum of SNR is observed for $k_1>6.25k_2$ $(k_2<0.16k_1)$, corresponding to trapping monostable potentials. In the central white area, which is for $0.16k_1<k_2<3.27k_1$, SNR and SPA have monotonic behavior as a function of the dimensionless noise intensity q/H.

strength of the force. Namely, the return force in the area located far from the equilibrium point should be much weaker than that close to the equilibrium point. For the potential of Eq. (3), the strength of the force changes in the points $x=\pm L$. For $k_1>6.25k_2$, this change is large enough and a maximum of SNR as a function of noise intensity is observed.

Such a shape of potential profile is responsible for system properties similar to those found in the dynamics of excitable systems, where the SR was also observed [1,37–39]. The excitable systems also have only one stable state. Under a small perturbation these systems relax quickly to the stable state. Conversely, a large (over threshold) perturbation switches the system to an excited state, which is unstable and decays to the stable state after a relatively long time. For the potential profile of Eq. (3), when $k_1 \gg k_2$ the system of Eq. (1) returns to the stable state relatively quickly if the perturbation is smaller than H. When the perturbation exceeds the value H, the system remains in the region $|x|>L$ for a relatively long period of time, because the return force now is weak. However, the similarities between our system and excitable systems are only qualitative. In fact, the equations describing excitable and threshold systems are different from Eq. (1).

Using the Laplace transform of the autocorrelation function [see Eq. (19)], we can obtain the SPA for the investigated monostable system. The plot of SPA as a function of the dimensionless input noise intensity is shown in Fig. 4. The parameters of the system for curves 1 and 2 in this figure are the same as in Fig. 2. For the potential profile 2 ($k_1=25$, $k_2=3$, $L=0.2$), theoretical and numerical results show a very good agreement (see red curve and black circles in Fig. 4). For the potential profile 1 ($k_1=20$, $k_2=1$, $L=0.1$; see Fig. 1), we obtain a little overestimation of the numerical values of SPA in comparison with the analytical results (see green curve and blue circles in Fig. 4). This should be ascribed to the strong variation in the slope of the potential profile around the point $|x|=L$, which causes a strong nonlinearity producing a large output signal. The results shown in Figs. 2 and 4 indicate that the linear-response theory, which provides exact results only for the case of harmonic potential, works very well with the considered nonlinear potential profile [Eq. (3)].

The reason of different behaviors of the SNR and SPA versus the noise intensity should be ascribed to the peculiarity of the trapping potential profile. Specifically, the presence in the potential profile of two regions with different slopes forces the Brownian particle to remain for a longer time in those regions characterized by low pendency ($|x|>L$). This physical picture corresponds to that obtained in bistable confining potential for conventional SR, even if the trapping potential profile is not confining [26]. This gives the nonmonotonic behavior of SNR. On the other hand, the SPA has a monotonic increasing behavior with increasing noise intensity, just because the trapping potential profile is not confining. In fact, the SPA has a nonmonotonic behavior in confining potential profiles as, for example, in the overdamped nonlinear oscillator [28–30].

The monostable system considered in Ref. [28] exhibits a nonmonotonic behavior of SPA as a function of the noise intensity, called by the authors "intrawell SR." The monostable potential used in Ref. [28] corresponds to the potential profile of the mixed system (see Fig. 3 in Ref. [29], and Ref. [30]) and to the confining potentials in Fig. 5 (pink shaded area), with $k_1 \ll k_2$ in Eq. (3). In Refs. [29,30], the SNR of this mixed system or the so-called confining potential shows monotonic behavior as a function of the noise

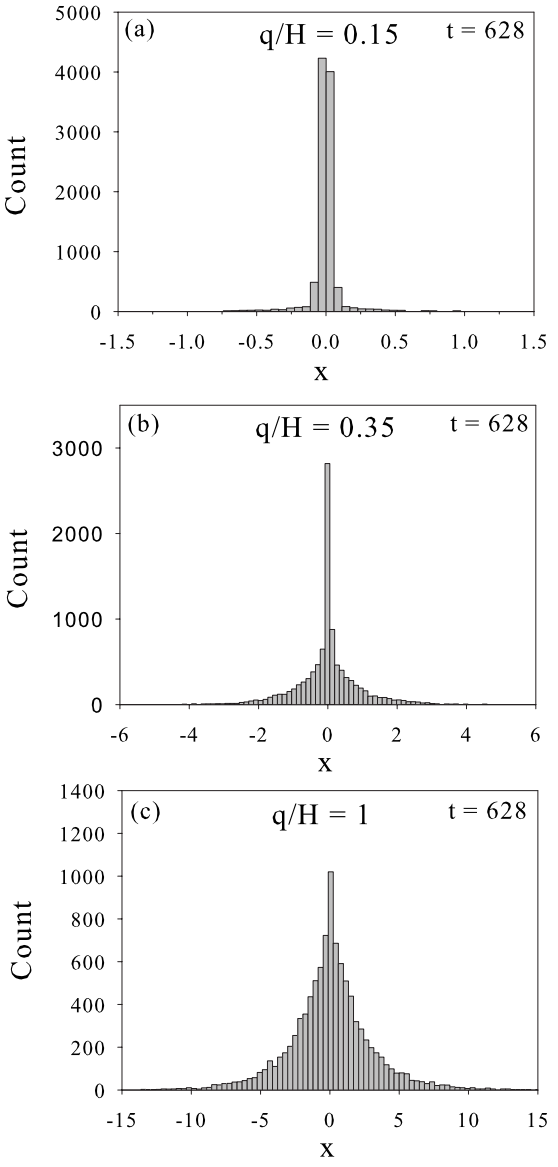

FIG. 6. PD for the position x of the Brownian particle moving along the trapping monostable potential profile 1 of Fig. 1 ($k_1=20$, $k_2=1$, $L=0.1$). The PD is shown at time $t=t_{max}=628$, for three different values of the noise intensity, namely, $q/H=0.15, 0.35, 1$. The first and third noise intensities correspond to small values of SNR, while the second value gives the maximum of SNR (see green solid line and blue circle in Fig. 2). Amplitude and frequency of the input periodical signal are $A=0.3$ and $\omega_0=0.1$, respectively.

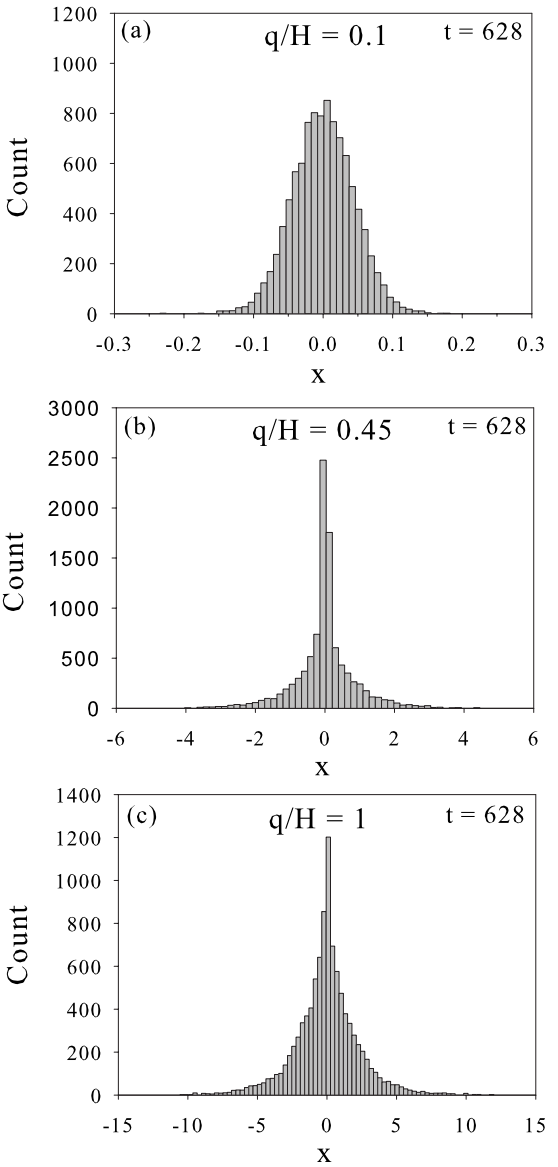

FIG. 7. PD for the position x of the Brownian particle moving along the trapping monostable potential profile 2 ($k_1=25$, $k_2=3$, $L=0.2$). The PD is shown at time $t=t_{max}=628$, for three different values of the noise intensity, namely, $q/H=0.1$, 0.45, 1. The first and third noise intensities correspond to small values of SNR, while the second value gives the maximum of SNR (see red solid line and black circle in Fig. 2). Amplitude and frequency of the input periodical signal are $A=0.3$ and $\omega_0=0.1$, respectively.

intensity. Moreover, in Ref. [30] other two potential profiles were investigated, namely, the so-called hard-soft nonlinear potential profile and a hybrid of two hard systems (see Eq. (52) and Figs. 5–9 in Ref. [30]). Both nonlinear systems show nonmonotonic behavior of SNR and SPA as a function of the noise intensity, with minima for SPA (called stochastic antiresonance) and maxima for SNR, or minimum and maximum of SPA depending on the values of the system parameters.

Analyzing the results obtained in Refs. [28–30] and in the present paper we conclude that in monostable overdamped systems the behavior of SNR and SPA can be very different, strongly depending on the shape of the potential profile. Specifically the shape of the trapping part of the potential profile (compare, for example, the potential in Fig. 1 of this paper with that in Fig. 7 of Ref. [30]) plays a crucial role in the appearance of the so-called stochastic antiresonance. In the monostable system investigated here [Eq. (3)], the parameter space (k_1, k_2) is divided into three nonoverlapping areas (see Fig. 5), namely, (i) for $k_2 > 3.27k_1$, maxima of SPA are observed in confining monostable potential profiles ($k_1 \ll k_2$); (ii) for $0.16k_1 < k_2 < 3.27k_1$, monotonic behavior both of SNR and SPA are observed; and (iii) for $k_2 < 0.16k_1$, maxima

of SNR are observed in trapping monostable potential profiles ($k_1 \gg k_2$).

To complete our analysis, we calculated at time $t=t_{max}=628$ the PD for the position x of the Brownian particle moving along the trapping monostable potential in Fig. 1. This time t_{max} is sufficiently long to ensure that the stationary probability distributions are established. For our numerical calculations of the PDs we choose as initial condition $x=0$ for the particle position and random values for the phase φ, uniformly distributed in the interval $[0,2\pi]$. Specifically, we show in Fig. 6 the PD for the potential profile 1, with $k_1=20$, $k_2=1$, $L=0.1$, at time $t=628$, for three different values of the noise intensity, namely, $q/H=0.15,0.35,1$. The first and third noise intensities correspond to small values of SNR, while the second value gives the maximum of SNR (see green solid line 1 and blue circle in Fig. 2). We note that at low noise intensity the particle is mostly confined around the minimum ($x=0$) of the potential profile 1, with few trajectories showing escape of the Brownian particle from the well toward regions with $|x|>L$. By increasing the noise intensity, more trajectories show escape from the well and, as a consequence, the probability distributions show fat tails. By increasing the noise intensity, the probability of finding the Brownian particle in the trap decreases, while the probability of finding the particle outside the trap increases. A particular noise level $\tilde{q}$ exists for which the above-mentioned probabilities are equal. In fact, by equating these probabilities, calculated using the stationary PDF of Eq. (13), we obtain

$$2N\frac{\tilde{q}}{k_1}(1-e^{-H/\tilde{q}})=2N\frac{\tilde{q}}{k_2}e^{-H/\tilde{q}}, \tag{24}$$

$$\frac{H}{\tilde{q}}=\ln\left(1+\frac{k_1}{k_2}\right). \tag{25}$$

From this equation and for potential profile 1 we find $\tilde{q}\simeq 0.33H$, which is very close to the value of q^* for which the SNR has a maximum in the trapping monostable potential profile 1.

In Fig. 7 we report the PD for potential profile 2 ($k_1=25$, $k_2=3$, $L=0.2$) at the same time $t=628$, for three different values of the noise intensity, namely, $q/H=0.1,0.45,1$. The first and third noise intensities correspond to small values of SNR, while the second value gives the maximum of SNR (see red solid line and black circle in Fig. 2). From Eq. (25) and for this potential profile we obtain $\tilde{q}\simeq 0.45H$, which coincides with the value of q^* for which the SNR has a maximum in the trapping monostable potential profile 2. The potential profile 2 produces a greater confinement. As a consequence, the PDs show a Gaussian behavior for very low noise intensity and, for higher noise intensities, tails less fat than those shown for potential profile 1.

IV. CONCLUSIONS

We studied the response of a trapping overdamped monostable system to a periodic driving force, in the presence of a white Gaussian noise source and for a piecewise linear potential. Two standard quantifiers of stochastic resonance phenomenon have been analyzed, namely, signal-to-noise ratio and spectral power amplification. The theoretical approach used is based on linear-response theory and Laplace transform technique. Exact analytical expressions, within the LRT, are obtained for SNR and SPA. Theoretical results are compared with numerical ones. We find nonmonotonic behavior of the signal-to-noise ratio as a function of the noise intensity, while the signal power amplification shows monotonic behavior versus the noise intensity. This different behavior of SNR and SPA, which depends on the peculiarity of the trapping potential profile, differs from conventional SR observed in bistable and multistable potential profiles, where both SNR and SPA show nonmonotonic behavior as a function of the noise intensity.

Understanding the effects of modulation of trapping potential profiles on the motion of a Brownian particle can be very important in optical and magneto-optical traps, superconducting resonators showing monostability, and quantum mesoscopic systems. Moreover, the optical trapping technique gives the possibility to generate a desirable landscape of the potential energy to study experimentally a micrometer-sized Brownian particle moving in a modulated trap.

ACKNOWLEDGMENTS

This work was supported by Russian Foundation for Basic Research (Project No. 08-02-01259). We acknowledge also support by MIUR and INFM-CNISM.

[1] L. Gammaitoni, P. Hänggi, P. Jung, and F. Marchesoni, Rev. Mod. Phys. **70**, 223 (1998).
[2] V. S. Anishchenko, V. V. Astakhov, A. B. Neiman, T. E. Vadivasova, and L. Schimansky-Geier, *Nonlinear Dynamics of Chaotic and Stochastic Systems* (Springer, Berlin, 2002).
[3] L. Gammaitoni, P. Hänggi, P. Jung, and F. Marchesoni, in *Stochastic Resonance*, edited by Peter Hänggi and Fabio Marchesoni, special issue of Eur. Phys. J. B **69**, 1 (2009).
[4] R. N. Mantegna and B. Spagnolo, Phys. Rev. E **49**, R1792 (1994).
[5] M. I. Dykman, T. Horita, and J. Ross, J. Chem. Phys. **103**, 966 (1995).
[6] S. Mitaim and B. Kosko, Proc. IEEE **86**, 2152 (1998).
[7] J. M. G. Vilar, R. V. Solé, and J. M. Rubí, Phys. Rev. E **59**, 5920 (1999).
[8] P. E. Greenwood, L. M. Ward, D. F. Russell, A. Neiman, and F. Moss, Phys. Rev. Lett. **84**, 4773 (2000).
[9] R. N. Mantegna, B. Spagnolo, and M. Trapanese, Phys. Rev. E **63**, 011101 (2000).
[10] P. Hänggi, ChemPhysChem **3**, 285 (2002).
[11] B. Spagnolo, M. Cirone, A. La Barbera, and F. de Pasquale, J. Phys.: Condens. Matter **14**, 2247 (2002).

[12] S. Zozor and P.-O. Amblard, IEEE Trans. Signal Process. **51**, 3177 (2003).
[13] D. Valenti, A. Fiasconaro, and B. Spagnolo, Physica A **331**, 477 (2004).
[14] R. N. Mantegna, B. Spagnolo, L. Testa, and M. Trapanese, J. Appl. Phys. **97**, 10E519 (2005).
[15] B. Spagnolo, S. Spezia, L. Curcio, N. Pizzolato, A. Fiasconaro, D. Valenti, P. Lo Bue, E. Peri, and S. Colazza, Eur. Phys. J. B **69**, 133 (2009).
[16] A. Fulinski, Phys. Rev. E **52**, 4523 (1995); Y. F. Jin, W. Xu, M. Xu, and T. Fang, J. Phys. A **38**, 3733 (2005); L. J. Ning and W. Xu, Physica A **382**, 415 (2007).
[17] J. F. Lindner, B. J. Breen, M. E. Wills, A. R. Bulsara, and W. L. Ditto, Phys. Rev. E **63**, 051107 (2001).
[18] N. G. Stocks, N. D. Stein, and P. V. E. McClintock, J. Phys. A **26**, L385 (1993).
[19] A. N. Grigorenko, S. I. Nikitin, and G. V. Roschepkin, Phys. Rev. E **56**, R4907 (1997).
[20] M. Evstigneev, V. Pankov, and R. H. Prince, J. Phys. A **34**, 2595 (2001).
[21] E. Segev, B. Abdo, O. Shtempluck, and E. Buks, Phys. Rev. B **77**, 012501 (2008).
[22] R. Di Leonardo, G. Ruocco, J. Leach, M. J. Padgett, A. J. Wright, J. M. Girkin, D. R. Burnham, and D. McGloin, Phys. Rev. Lett. **99**, 010601 (2007).
[23] Y. Seol, K. Visscher, and D. B. Walton, Phys. Rev. Lett. **93**, 160602 (2004).
[24] Y. Deng, J. Bechhoefer, and N. R. Forde, J. Opt. A, Pure Appl. Opt. **9**, S256 (2007).
[25] G. Volpe, S. Perrone, J. M. Rubi, and D. Petrov, Phys. Rev. E **77**, 051107 (2008).
[26] E. Heinsalu, M. Patriarca, and F. Marchesoni, Eur. Phys. J. B **69**, 19 (2009).
[27] B. McNamara and K. Wiesenfeld, Phys. Rev. A **39**, 4854 (1989).
[28] M. Evstigneev, P. Reimann, V. Pankov, and R. H. Prince, EPL **65**, 7 (2004).
[29] N. V. Agudov and A. V. Krichigin, Int. J. Bifurcation Chaos **18**, 2833 (2008).
[30] N. V. Agudov and A. V. Krichigin, Radiophys. Quantum Electron. **51**, 812 (2008).
[31] H. Risken, *The Fokker-Planck Equation: Methods of Solution and Applications* (Springer-Verlag, Berlin, 1989).
[32] J. D. Atkinson and T. K. Caughey, Int. J. Non-Linear Mech. **3**, 137 (1968).
[33] N. V. Agudov and A. N. Malakhov, Radiophys. Quantum Electron. **36**, 97 (1993).
[34] A. N. Malakhov and A. L. Pankratov, Physica A **229**, 109 (1996).
[35] V. Privman and H. L. Frisch, J. Chem. Phys. **94**, 8216 (1991).
[36] D. A. Leahy *et al.*, Astrophys. J. **266**, 160 (1983).
[37] A. Longtin, J. Stat. Phys. **70**, 309 (1993).
[38] A. Longtin and D. R. Chialvo, Phys. Rev. Lett. **81**, 4012 (1998).
[39] B. Lindner, J. García-Ojalvo, A. Neiman, and L. Schimansky-Geier, Phys. Rep. **392**, 321 (2004).